

Received December 12, 2021, accepted January 5, 2022, date of publication January 7, 2022, date of current version January 18, 2022.

Digital Object Identifier 10.1109/ACCESS.2022.3141492

Distributed Finite Memory Estimation From Relative Measurements for Multiple-Robot Localization in Wireless Sensor Networks

YEONG JUN KIM¹, HYUN HO KANG¹, SANG SU LEE¹, JUNG MIN PAK², (Member, IEEE), AND CHOON KI AHN¹, (Senior Member, IEEE)

¹School of Electrical Engineering, Korea University, Seongbuk-gu, Seoul 02841, Republic of Korea

²Department of Electrical Engineering, Wonkwang University, Iksan-si, Jeollabuk-do 54538, Republic of Korea

Corresponding authors: Jung Min Pak (destin11@wku.ac.kr) and Choon Ki Ahn (hironaka@korea.ac.kr)

This work was supported in part by the National Research Foundation of Korea (NRF) funded by the Korean Government (MSIT) under Grant 2020R1F1A1072428, and in part by the National Research Foundation of Korea (NRF) funded by the Korean Government (MSIT) under Grant 2020R1A2C1005449.

ABSTRACT Mobile robot localizations have been extensively studied, and various algorithms for multiple-robot localization have been developed. However, existing methods for multiple-robot localization often exhibit poor performance under harsh conditions, such as missing measurements and sudden appearance of obstacles. To overcome this problem, this paper proposes a novel method for multiple-robot localization in wireless sensor networks. The proposed method is theoretically based on the finite memory estimation and utilizes relative distance and angle measurements between robots. Thus, the proposed method is referred to as distributed finite memory estimation from relative measurements (DFMERM). Due to the finite memory structure, the DFMERM has inherent robustness against computational and modeling errors. Moreover, the novel distributed localization method using relative measurements shows the robustness against missing measurements. Robust DFMERM localization performance is experimentally demonstrated using multiple mobile robots under the harsh conditions.

INDEX TERMS Distributed localization, finite memory estimation, mobile robot, relative measurements, wireless sensor networks.

I. INTRODUCTION

Real-time locating systems (RTLS) based on wireless sensor networks (WSN) are popular in various industrial fields, such as smart factories, public facilities, and logistics facilities [1]–[7]. However, RTLS suffer from localization failure due to missing measurements [8], [9], which are caused by communication and sensor errors. Moreover, using lightweight and low-cost sensors in RTLS exacerbates these problems. Thus, a novel localization algorithm that can cope with the missing measurement problem is required.

Localization algorithms based on WSN can be categorized into two groups: the centralized and distributed algorithms. The centralized algorithms process data from all mobile nodes in a single server computer. If the number of mobile devices is large, the data from the node to the server may

cause bottlenecks and data loss [10]–[12]. The distributed algorithms can solve this problem by processing the data in distributed multiple servers. Various algorithms for multiple-robot localization have been developed [13]–[24], and especially, in [13], the problem of the distributed localization of multiple mobile robots when the communication link with neighboring nodes is temporarily lost was studied. In addition, machine learning (ML)-based localization algorithms for WSNs were developed to obtain an accurate location and minimize the adverse effects of internal or external factors [25]. A ML-based localization algorithm, the Bayesian technique with sequential Monte Carlo was used to estimate the location of unknown nodes [26]. The Bayesian compressive sensing technique for adaptive localization was developed to estimate the target locations, considering environmental noise variance [27]. The variational Bayesian interface based iterative technique was introduced to recover sparse signals and faulty prior information [28]. However,

The associate editor coordinating the review of this manuscript and approving it for publication was Stefano Scanzio¹.

these algorithms are based on infinite impulse response (IIR) estimation, and they may exhibit estimation divergence due to the accumulation of computational or modeling errors.

IIR estimation is familiar to engineers because the Kalman filter (KF) is one of the most commonly known IIR estimation algorithms. Different versions of KF have been studied and applied to diverse engineering problems, including the distributed localization [14], [16], [17]. However, KFs suffer from filter divergence, which is caused by the accumulation of computational or modeling errors. To overcome this problem, finite memory estimation (FME) algorithms [5], [12], [29]–[37] that use only recent finite measurements have been studied. Distributed FME were studied in [32]–[34], and they exhibited better robustness than those of distributed IIR filters. However, these studies were limited to the problem of estimating the location of a single robot in a WSN.

In this paper, we propose a novel distributed FME algorithm for multiple-robot localization; thus, it can estimate the pose (i.e., position and heading angle) of all individual robots in a WSN. The proposed FME is referred to as the distributed FME from relative measurements (DFMERM). The technique for refining sensor measurements proposed in our previous study [31] is evolved and extended to the distributed multiple-robot localization problem. The measurements of relative distance and heading angle between robots are transmitted to neighbors through robot-to-robot direct communication, which facilitates distributed localization. In addition, the novel measurement redefining technique proposed in this paper helps the localization algorithm to cope with missing measurements. Lastly, the finite memory (FM) structure makes the DFMERM robust against the computational errors caused by the missing measurements. Superior DFMERM robustness and reliable localization performance are experimentally demonstrated using the multiple mobile robots under harsh conditions, including missing measurements and sudden appearance of an obstacle. The main contributions and novelty of this paper can be summarized as follows:

- 1) The proposed DFMERM is the first distributed FME algorithm that is capable of multiple-robot localization; existing distributed FME algorithms [32]–[34] are only available for single-robot localization.
- 2) We designed a novel distributed multiple-robot localization system, in which a few robots are equipped with expensive sensors that are capable of absolute positioning, whereas the majority of robots have low-cost sensors that can only measure relative distance and bearing between robots. This reduces the implementation cost of multiple-robot localization systems, and the cost reduction effect increases as the number of robots increases.
- 3) A novel FME algorithm to overcome the missing measurement problem was proposed. The missing measurements were replaced by the predicted measurements, and the measurement equation was redefined.

The novel FME was derived using the new state-space model based on redefined measurements. The resulting DFMERM experimentally exhibited robustness against missing measurements.

- 4) The proposed DFMERM exhibited superior localization performance that is better than that of the conventional IIR localization algorithm. The DFMERM was more robust than the distributed IIR filter against not only the missing measurements but also sudden appearance of an obstacle because the DFMERM has the FM filter structure, which is inherently robust against modeling and computational errors.

The remainder of this paper is organized as follows. Section II describes scheme of the distributed multiple-robot localization using relative measurements. Section III derives the DFMERM by utilizing the Frobenius norm and Lagrange multiplier method. Section IV presents the results of experiments using six mobile robots. Finally, conclusions are drawn in Section V.

II. SCHEME OF DISTRIBUTED MULTIPLE-ROBOT LOCALIZATION USING RELATIVE MEASUREMENTS

We consider a situation in which multiple mobile robots are in a 2-dimensional (2D) indoor space. We divide the robots into two groups, Groups A and B. Group A is composed of a few robots equipped with high-resolution sensors that can obtain their positions. Group B has many robots equipped with low-cost sensors that can only measure relative distance and/or bearing. This paper focuses on the localization of multiple robots in Group B using the relative measurements.

A. KINEMATIC MODEL

The state and control input of the i -th robot at a discrete time step k are defined as follows:

$$s_{i,k} = [p_{i,k}^T \quad \theta_{i,k}]^T, \quad (1)$$

$$u_{i,k} = [v_{i,k}^l \quad v_{i,k}^\theta]^T, \quad (2)$$

where $p_{i,k} = [x_{i,k} \ y_{i,k}]^T$, with positions $x_{i,k}$ and $y_{i,k}$ being in the x - and y -axes, respectively. $\theta_{i,k}$ is the heading angle of the i -th robot with respect to the x -axis, and $v_{i,k}^l$ and $v_{i,k}^\theta$ are the linear and angular velocities of the i -th robot. We consider the nonholonomic unicycle kinematic model of the mobile robot described in Fig. 1. The relationship between $s_{i,k}$ and $s_{i,k+1}$ with time variation Δt is defined as [8], [31]

$$s_{i,k+1} = f_{i,k}(s_{i,k}, u_{i,k}) + \omega_{i,k} \\ \triangleq s_{i,k} + \bar{f}_{i,k} u_{i,k} \Delta t + \omega_{i,k}, \quad (3)$$

where $\omega_{i,k}$ is process noise vector of the i -th robot at time k , and $\bar{f}_{i,k}$ is defined as

$$\bar{f}_{i,k} = \begin{bmatrix} \cos \theta_{i,k} & 0 \\ \sin \theta_{i,k} & 0 \\ 0 & 1 \end{bmatrix}. \quad (4)$$

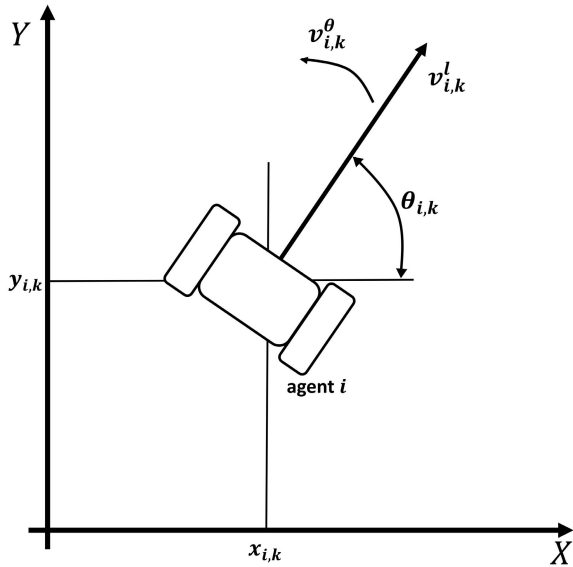


FIGURE 1. Description of kinematic model.

B. MEASUREMENT

We consider a directed graph, which is denoted as $\mathcal{G} = (\mathcal{K}, \mathcal{E})$, where \mathcal{K} and \mathcal{E} are the set of robots and links, respectively. The number of robots is $M = \|\mathcal{K}\|$. In \mathcal{E} , the direction from robot j to i is denoted by (i, j) . The neighbors for robot i are defined as $\mathcal{N}_i = \{j : (i, j) \in \mathcal{E}\}$. Moreover, robot i can fetch the estimated state of Group A neighboring robots through directed communication. Accordingly, $J_i = |\mathcal{N}_i|$ denotes the number of Group A i -th neighbors. We assume that the i -th robot can obtain the estimated positions of neighbors at every sampling time. The description of the measurement is shown in Fig. 2. The measurement at time k of the i -th robot is

$$z_{i,k} = h_{i,k}(s_{i,k}) + \pi_{i,k},$$

$$\triangleq \begin{bmatrix} d_{i,k}^1 & \eta_{i,k}^1 & d_{i,k}^2 & \eta_{i,k}^2 & \dots & d_{i,k}^{J_i} & \eta_{i,k}^{J_i} & \theta_{i,k} \end{bmatrix}^T + \pi_{i,k}, \quad (5)$$

where

$$d_{i,k}^j = \|\hat{p}_{j,k} - p_{i,k}\|,$$

$$\eta_{i,k}^j = \tau_{i,k}^j - \theta_{i,k},$$

$$= \arctan\left(\frac{\Delta y_{i,k}^j}{\Delta x_{i,k}^j}\right) - \theta_{i,k},$$

$$\Delta x_{i,k}^j = \begin{bmatrix} 1 & 0 \end{bmatrix} \hat{p}_{j,k} - \begin{bmatrix} 1 & 0 \end{bmatrix} p_{i,k},$$

$$\Delta y_{i,k}^j = \begin{bmatrix} 0 & 1 \end{bmatrix} \hat{p}_{j,k} - \begin{bmatrix} 0 & 1 \end{bmatrix} p_{i,k}, \quad (6)$$

and $\pi_{i,k}$ is the measurement noise vector of the i -th robot at time k . $\hat{p}_{j,k}$ is the estimated two-dimensional position of the j -th robot at time k , $d_{i,k}^j$ denotes the center distance between the i -th and j -th robots at time k , $\eta_{i,k}^j$ denotes the angle from the heading of the i -th robot to the j -th robot at time k , and

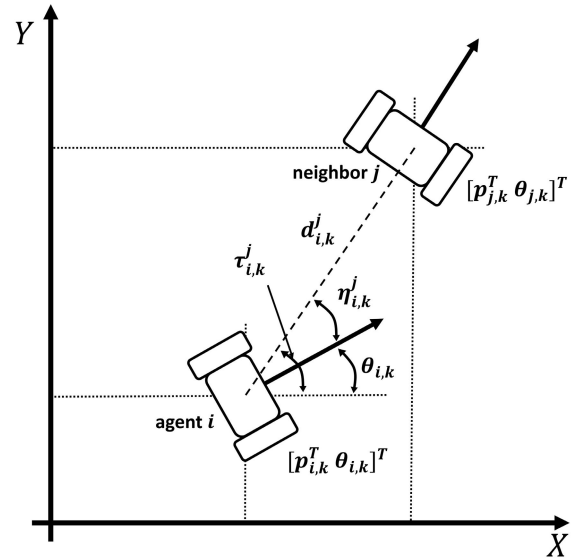


FIGURE 2. Description of measurement with neighbor $j \in [1, J_i]$.

$\tau_{i,k}^j$ denotes the angle from the x-axis to the j -th robot at time k with respect to the i -th robot. $\Delta x_{i,k}^j$ and $\Delta y_{i,k}^j$ are the differences between i -th and j -th robots on the x- and y-axes, respectively. If the i -th robot does not have a link with the j -th robot, then the measurements $d_{i,k}^j$ and $\eta_{i,k}^j$ are set to zero.

C. REDEFINED MEASUREMENT

As the number of robots increases during position estimation for the multiple mobile robot system, temporal failure of the communication link occurs more frequently, which makes it difficult to estimate the robot positions accurately, and it may cause a significant failure in the estimation [13]. In this case, the estimation algorithm needs to handle temporal missing communication. Therefore, we rewrite (5) using previously stored estimated values [31]:

$$\bar{z}_{i,k} = \gamma_{i,k} h_{i,k}(s_{i,k}) + (I_{2J_i+1} - \gamma_{i,k}) h_{i,k}(\check{s}_{i,k}) + \bar{\pi}_{i,k},$$

$$= \begin{cases} h_{i,k}(\check{s}_{i,k}) + \bar{\pi}_{i,k}, & \text{missing measurement} \\ h_{i,k}(s_{i,k}) + \bar{\pi}_{i,k}, & \text{else} \end{cases} \quad (7)$$

where $\check{s}_{i,k} = f(\hat{s}_{i,k-1}, u_{i,k-1})$ is the predicted value using the previous estimated state $\hat{s}_{i,k-1}$, and $\bar{\pi}_{i,k}$ is the redefined measurement noise vector of the i -th robot at time k . I_{2J_i+1} is the identity matrix size of $2J_i+1$, and $\gamma_{i,k}$ is a diagonal matrix consisting of a binary value at the current step k . It is set to 0 when a measurement is missing; otherwise, it is 1. $\gamma_{i,k}$ can also be used to account for transient errors in the sensor.

III. DISTRIBUTED FINITE MEMORY ESTIMATION FROM RELATIVE MEASUREMENT

This section describes the DFMERM for estimating the state of a problem formulated in Section II. We consider the robot index i as the filtering number of all robots. Utilizing the

nonlinear functions (3) and (7), the discrete-time system models can be represented by the process and measurement equations:

$$s_{i,k+1} = f_{i,k}(s_{i,k}, u_{i,k}) + w_{i,k}, \quad (8)$$

$$\begin{aligned} \bar{z}_{i,k} &= \gamma_{i,k} h_{i,k}(s_{i,k}) \\ &+ (I_{2J_i+1} - \gamma_{i,k}) h_{i,k}(\check{s}_{i,k}) + \bar{\pi}_{i,k}, \end{aligned} \quad (9)$$

where $f_{i,k}(s_{i,k}, u_{i,k})$ and $h_{i,k}(s_{i,k})$ are nonlinear functions. We assume that $w_{i,k}$ and $\bar{\pi}_{i,k}$ are zero-mean white Gaussian noise vectors. The noise covariances of the i -th robot with respect to $w_{i,k}$ and $\bar{\pi}_{i,k}$ are defined as $\mathcal{Q}_i = E[w_{i,k} w_{i,k}^T]$ and $\mathcal{R}_i = E[\bar{\pi}_{i,k} \bar{\pi}_{i,k}^T]$, where $E[\cdot]$ is the expectation operator.

Define the Jacobian matrices of $f_{i,k}(s_{i,k}, u_{i,k})$ and $h_{i,k}(s_{i,k})$ around $s_{i,k} = \hat{s}_{i,k}$ and $s_{i,k} = \check{s}_{i,k}$ as

$$\hat{F}_{i,k} = \left. \frac{\partial f_{i,k}(s_{i,k}, u_{i,k})}{\partial s_{i,k}} \right|_{s=\hat{s}_{i,k}}, \quad (10)$$

$$\hat{H}_{i,k} = \left. \frac{\partial h_{i,k}(s_{i,k})}{\partial s_{i,k}} \right|_{s=\hat{s}_{i,k}}, \quad (11)$$

$$\check{H}_{i,k} = \left. \frac{\partial h_{i,k}(s_{i,k})}{\partial s_{i,k}} \right|_{s=\check{s}_{i,k}}. \quad (12)$$

Utilizing the Jacobian matrices, (10) (11) and (12), the linearization of nonlinear system (8) and (9) are defined as follows:

$$s_{i,k+1} = f_{i,k}(\hat{s}_{i,k}, u_{i,k}) + \hat{F}_{i,k}(s_{i,k} - \hat{s}_{i,k}) + w_{i,k}, \quad (13)$$

$$\begin{aligned} \bar{z}_{i,k} &= \gamma_{i,k}(h_{i,k}(\hat{s}_{i,k}) + \hat{H}_{i,k}(s_{i,k} - \hat{s}_{i,k})) \\ &+ (I_{2J_i+1} - \gamma_{i,k})(h_{i,k}(\check{s}_{i,k}) + \check{H}_{i,k}(s_{i,k} - \check{s}_{i,k})) \\ &+ \bar{\pi}_{i,k}. \end{aligned} \quad (14)$$

We simplify linearized system (13) and (14) as follows:

$$s_{i,k+1} = \hat{A}_{i,k} s_{i,k} + \mathcal{A}_{i,k} + w_{i,k}, \quad (15)$$

$$\bar{z}_{i,k} = \mathcal{B}_{i,k} s_{i,k} + \mathcal{C}_{i,k} + \bar{\pi}_{i,k}, \quad (16)$$

where

$$\begin{aligned} \hat{A}_{i,k} &= f_{i,k}(\hat{s}_{i,k}, u_{i,k}) - \hat{F}_{i,k} \hat{s}_{i,k}, \\ \mathcal{B}_{i,k} &= \gamma_{i,k} \hat{H}_{i,k} + (I_{2J_i+1} - \gamma_{i,k}) \check{H}_{i,k}, \\ \mathcal{C}_{i,k} &= \gamma_{i,k}(h_{i,k}(\hat{s}_{i,k}) - \hat{H}_{i,k} \hat{s}_{i,k}) \\ &+ (I_{2J_i+1} - \gamma_{i,k})(h_{i,k}(\check{s}_{i,k}) - \check{H}_{i,k} \check{s}_{i,k}). \end{aligned} \quad (17)$$

The proposed algorithm in discrete-time space requires recent N measurements, where N denotes horizon size. To stack N measured values, the linearized systems (15) and (16) are utilized. An equation starting from $\bar{z}_{i,k}$ with $n \in [1, N]$ is

$$\begin{aligned} \bar{z}_{i,k+n} &= \mathcal{B}_{i,k+n} \mathcal{F}_i(0, n) s_{i,k} \\ &+ \mathcal{B}_{i,k+n} \mathcal{F}_i(1, n) (\mathcal{A}_{i,k} + w_{i,k}) \\ &+ \mathcal{B}_{i,k+n} \mathcal{F}_i(2, n) (\mathcal{A}_{i,k+1} + w_{i,k+1}) \\ &\vdots \\ &+ \mathcal{B}_{i,k+n} \mathcal{F}_i(n-1, n) (\mathcal{A}_{i,k+n-2} + w_{i,k-2}) \\ &+ \mathcal{B}_{i,k+n} \mathcal{F}_i(n, n) (\mathcal{A}_{i,k+n-1} + w_{i,k+n-1}) \\ &+ \mathcal{C}_{i,k+n} + \bar{\pi}_{i,k+n}, \end{aligned} \quad (18)$$

where

$$\mathcal{F}_i(a, b) = \begin{cases} \prod_{n=a}^{b-1} \hat{F}_{i,k+b-n-1} & \text{if } a < b, a \geq 0, b > 0; \\ I & \text{if } a = b; \\ 0 & \text{otherwise.} \end{cases}$$

From (18), the stacked matrix of filter i with the number of N is established as follows:

$$\begin{aligned} Z_{i,k+N} &= \Xi_{i,k+N} s_{i,k} + \Lambda_{i,k+N} (\Gamma_{i,k+N} + W_{i,k+N}) \\ &\quad + \Psi_{i,k+N} + \Phi_{i,k+N}, \end{aligned} \quad (19)$$

where

$$\begin{aligned} Z_{i,k+N} &= \begin{bmatrix} \bar{z}_{i,k+1} \\ \bar{z}_{i,k+2} \\ \vdots \\ \bar{z}_{i,k+N} \end{bmatrix}, \\ \Xi_{i,k+N} &= \begin{bmatrix} \mathcal{B}_{i,k+1} \mathcal{F}(0, 1) \\ \mathcal{B}_{i,k+2} \mathcal{F}(0, 2) \\ \vdots \\ \mathcal{B}_{i,k+N} \mathcal{F}(0, N) \end{bmatrix}, \\ \Lambda_{i,k+N} &= \begin{bmatrix} \mathcal{B}_{i,k+1} \mathcal{F}(1, 1) & 0 & \cdots & 0 \\ \mathcal{B}_{i,k+2} \mathcal{F}(1, 2) & \mathcal{B}_{i,k+2} \mathcal{F}(2, 2) & \cdots & 0 \\ \vdots & \vdots & \ddots & \vdots \\ \mathcal{B}_{i,k+N} \mathcal{F}(1, N) & \mathcal{B}_{i,k+N} \mathcal{F}(2, N) & \cdots & \mathcal{B}_{i,k+N} \mathcal{F}(N, N) \end{bmatrix}, \\ \Gamma_{i,k+N} &= [\mathcal{A}_{i,k}^T \quad \mathcal{A}_{i,k+1}^T \quad \cdots \quad \mathcal{A}_{i,k+N-1}^T]^T, \\ \Psi_{i,k+N} &= [\mathcal{C}_{i,k+1}^T \quad \mathcal{C}_{i,k+2}^T \quad \cdots \quad \mathcal{C}_{i,k+N}^T]^T, \\ W_{i,k+N} &= [w_{i,k}^T \quad w_{i,k+1}^T \quad \cdots \quad w_{i,k+N-1}^T]^T, \\ \Phi_{i,k+N} &= [\bar{\pi}_{i,k+1}^T \quad \bar{\pi}_{i,k+2}^T \quad \cdots \quad \bar{\pi}_{i,k+N}^T]^T. \end{aligned} \quad (20)$$

To obtain the result $\hat{s}_{i,k+N}$ in the DFMERM filtering algorithm, we utilize the relationship between $s_{i,k}$ and $s_{i,k+N}$. Using $\Gamma_{i,k+N}$, $W_{i,k+N}$, and (15), and $s_{i,k+N}$ is obtained as follows:

$$s_{i,k+N} = \mathcal{F}_i(0, N) s_{i,k} + \Omega_{i,k+N} (\Gamma_{i,k+N} + W_{i,k+N}), \quad (21)$$

where

$$\Omega_{i,N} = [\mathcal{F}(1, N) \quad \mathcal{F}(2, N) \quad \cdots \quad \mathcal{F}(N, N)]. \quad (22)$$

We assume the systems have an unbiased condition to obtain gains. The state estimator algorithm with the filtering index i is defined as

$$\hat{s}_{i,k+N} = \mathcal{Q}_{i,k+N} Z_{i,k+N} + \mathcal{O}_{i,k+N} \Gamma_{i,k+N}, \quad (23)$$

where $Q_{i,k+N}$ and $O_{i,k+N}$ are the gain matrices, and the appropriate gain values are selected to estimate the state $\hat{s}_{i,k+N}$. By substituting (19) into (23) and subtracting (21) from both sides, the following equation can be derived:

$$\begin{aligned} \hat{s}_{i,k+N} &= (Q_{i,k+N} \Xi_{i,k+N} - \mathcal{F}_i(0, N))s_{i,k} \\ &\quad + (Q_{i,k+N} \Lambda_{i,k+N} - \Omega_{i,k+N})(\Gamma_{i,k+N} + W_{i,k+N}) \\ &\quad + Q_{i,k+N}(\Psi_{i,k+N} + \Phi_{i,k+N}) \\ &\quad + O_{i,k+N}\Gamma_{i,k+N} \\ &\quad + s_{i,k+N}. \end{aligned} \quad (24)$$

To derive unbiasedness in the condition defined as $E[s_{i,k+N}] = E[\hat{s}_{i,k+N}]$, the expectation of the above equation is given as follows:

$$\begin{aligned} E[\hat{s}_{i,k+N}] &= E[s_{i,k+N}] \\ &\quad + (Q_{i,k+N} \Xi_{i,k+N} - \mathcal{F}_i(0, N))E[s_{i,k}] \\ &\quad + (Q_{i,k+N} \Lambda_{i,k+N} - \Omega_{i,k+N} + O_{i,k+N})\Gamma_{i,k+N} \\ &\quad + Q_{i,k+N}\Psi_{i,k+N}, \end{aligned} \quad (25)$$

where $\Phi_{i,k+N}$ and $W_{i,k+N}$ constituting $\bar{\pi}_{i,k}$ and $w_{i,k}$ are zero when the expectation is calculated. The conditions for the gain matrices can be obtained from (25) as follows:

$$Q_{i,k+N} \Xi_{i,k+N} - \mathcal{F}_i(0, N) = 0, \quad (26)$$

$$\begin{aligned} (Q_{i,k+N} \Lambda_{i,k+N} - \Omega_{i,k+N} + O_{i,k+N})\Gamma_{i,k+N} \\ + Q_{i,k+N}\Psi_{i,k+N} = 0. \end{aligned} \quad (27)$$

To find the gains $Q_{i,k+N}$ and $O_{i,k+N}$ in (26) and (27), we set the appropriate optimization problem. Set the following cost function using the Frobenius norm defined as $\|\cdot\|_F$:

$$J_{i,k+N} = \frac{1}{2} \|Q_{i,k+N}\|_F^2. \quad (28)$$

We use the Lagrange multiplier method to minimize the cost function. The Lagrange multiplier defined as Θ is used to solve the cost function. Thus, we can define the following function:

$$\begin{aligned} \mathcal{L}_{i,k+N} &= \frac{1}{2} \|Q_{i,k+N}\|_F^2 \\ &\quad - \Theta^T (Q_{i,k+N} \Xi_{i,k+N} - \mathcal{F}_i(0, N)) \\ &= \frac{1}{2} \text{tr}[Q_{i,k+N}^T Q_{i,k+N}] \\ &\quad - \Theta^T (Q_{i,k+N} \Xi_{i,k+N} - \mathcal{F}_i(0, N)). \end{aligned} \quad (29)$$

In this case, the optimization problem can be solved to obtain the gain $Q_{i,k+N}$ when the partial derivative of $\mathcal{L}_{i,k+N}$ with respect to $Q_{i,k+N}$ equals zero. Then, $Q_{i,k+N}$ is obtained as follows:

$$Q_{i,k+N} = \Theta^T \Xi_{i,k+N}^T. \quad (30)$$

By substituting (30) into (26):

$$\Theta^T = \mathcal{F}_i(0, N)(\Xi_{i,k+N}^T \Xi_{i,k+N})^{-1}.$$

Algorithm 1 DFMERM

Input: $N, \mathcal{G}, \mathcal{N}_i$

while new data exists **do**

for all i -th robots, $i \in \mathcal{K}$ **do**

Get $\hat{p}_{j,k}$ from $\mathcal{N}_i = \{j : (i, j) \in \mathcal{E}\}$

Determine Jacobian matrices $\hat{F}_{i,k}$, $\hat{H}_{i,k}$, and $\check{H}_{i,k}$

if $z_{i,k}$ is available **then**

$\bar{z}_{i,k} = h_{i,k}(s_{i,k}) + \bar{\pi}_{i,k}$ with $\gamma_{i,k} = 1$

else

$\bar{z}_{i,k} = h_{i,k}(\check{s}_{i,k}) + \bar{\pi}_{i,k}$ with $\gamma_{i,k} = 0$

end if

Stack redefined measurement $\bar{z}_{i,k}$

if $k > N, k = 1, 2, \dots$ **then**

for $n \in [1, N]$ **do**

Construct $Z_{i,k+N}$ with $\bar{z}_{i,k+n}$

Construct $\Gamma_{i,k+N}$ with $\mathcal{A}_{i,k+n-1}^T$

Construct $\Xi_{i,k+N}$ with $\mathcal{B}_{i,k+n}\mathcal{F}(0, n)$

Construct $\Lambda_{i,k+N}$ with $\mathcal{B}_{i,k+n}\mathcal{F}(n, n)$

Construct $\Psi_{i,k+N}$ with $\mathcal{C}_{i,k+n-1}^T$

Optimize the cost function $J_{i,k+N}$

Obtain gain matrices $Q_{i,k+N}$ and $O_{i,k+N}$

Calculate the estimated state

$$\begin{aligned} \hat{s}_{i,K+N} &= Q_{i,k+N}Z_{i,k+N} \\ &\quad + O_{i,k+N}\Gamma_{i,k+N} \end{aligned}$$

end for

end if

end for

end while

return $\hat{s}_{i,K+N}$

Therefore, the gain matrix $Q_{i,k+N}$ and $O_{i,k+N}$ are arranged as follows.

$$\begin{aligned} Q_{i,k+N} &= \mathcal{F}_i(0, N)(\Xi_{i,k+N}^T \Xi_{i,k+N})^{-1} \Xi_{i,k+N}^T, \\ O_{i,k+N} &= \Omega_{k+N} \\ &\quad - \mathcal{F}_i(0, N)(\Xi_{i,k+N}^T \Xi_{i,k+N})^{-1} \Xi_{i,k+N}^T \Lambda_{i,k+N} \\ &\quad - \mathcal{F}_i(0, N)(\Xi_{i,k+N}^T \Xi_{i,k+N})^{-1} \Xi_{i,k+N}^T \Psi_{i,k+N} \Gamma_{i,k+N}^{-1}. \end{aligned} \quad (31)$$

The estimated state $\hat{s}_{i,k+N}$ from applying the gain matrix $Q_{i,k+N}$ and $O_{i,k+N}$ is obtained as follows:

$$\begin{aligned} \hat{s}_{i,k+N} &= \left(\mathcal{F}_i(0, N)(\Xi_{i,k+N}^T \Xi_{i,k+N})^{-1} \Xi_{i,k+N}^T \right) Z_{i,k+N} \\ &\quad + \left(\Omega_{i,k+N} - \mathcal{F}_i(0, N)(\Xi_{i,k+N}^T \Xi_{i,k+N})^{-1} \Xi_{i,k+N}^T \Lambda_{i,k+N} \right. \\ &\quad \left. - \mathcal{F}_i(0, N)(\Xi_{i,k+N}^T \Xi_{i,k+N})^{-1} \Xi_{i,k+N}^T \Psi_{i,k+N} \Gamma_{i,k+N}^{-1} \right) \Gamma_{i,k+N}. \end{aligned} \quad (32)$$

Remark 1: If there is a high noise effect that is not covered in noise covariances in the system, the iterative estimation



FIGURE 3. Robots in the experiment in the case of constant maneuvering: robots 1 and 2 are in Group A; their positions are estimated in a 2D plane in advance. Other robots are in Group B that measure the relative measurement, and the directional arrows represent information transmission links.

algorithm does not work properly. However, using the filter of the FM structure, the noise, which has a significant effect on the system, is canceled after N sampling times. Moreover, the FM structure algorithm can achieve better convergence to the reference in such a situation.

Remark 2: In the DFMERM, the horizon size should be carefully selected. The computational cost increases with horizon size. However, the noise-ignoring performance increases with horizon size. It is important to set an appropriate horizon size to trade off between computational cost and noise ignoring performance.

Remark 3: The DFMERM does not consider noise statistics. Thus, the DFMERM guarantees robustness against incorrect noise information. Moreover, obtaining the gain matrix by minimizing the Frobenius norm of the filter can reduce the error caused by mismodeling and an undefined noise effect.

IV. EXPERIMENT

In this section, the experiment for the distributed localization of multiple mobile robots is performed in the real world. The information, such as friction and slipping on the ground, are undefined in the experiment. We implemented the DFMERM and distributed IIR filter with ROBOTIS's TurtleBot3 Burger mobile robot platform. We used six robots in the experiment, and the network topology is shown in Fig. 3. A LiDAR scanner was used for relative measurement. We investigated two practical scenarios. Notably, the distributed FM estimation algorithm proposed in [32]–[34] cannot be applied to the experiment because they estimate only one target state.

A. MISSING MEASUREMENT CASE

The temporal sensor process delay and communication error can occur in real-world situations, and this fault should be addressed to perform the task successfully. During the experiment, 100 measurements were collected with

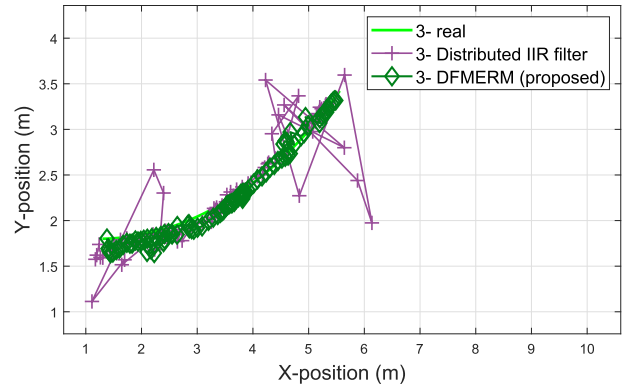


FIGURE 4. Robot 3 trajectory in the case of missing measurement.

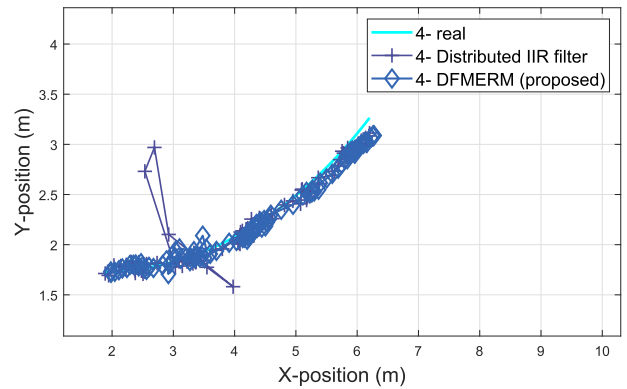


FIGURE 5. Robot 4 trajectory in the case of missing measurement.

$\Delta t = 1.5$ (s), $v_{i,k}^l = 0.03$ (m/s), and $v_{i,k}^\theta = 0.2$ (rad/s). We considered a missing measurement scenario with the following time step: robot 3 at times $29 \leq k \leq 33$ and $80 \leq k \leq 86$, robot 4 at times $29 \leq k \leq 33$, robot 5 at times $29 \leq k \leq 33$ and $75 \leq k \leq 79$, and robot 6 at times $29 \leq k \leq 33$ and $75 \leq k \leq 79$. The initial states of 1-st, 2-nd, \dots , 6-th robots are given as $[0.6 \ 1.8 \ 0]^T$, $[1.8 \ 1.2 \ 0]^T$, $[1.2 \ 1.8 \ 0]^T$, $[1.8 \ 1.8 \ 0]^T$, $[0.6 \ 1.2 \ 0]^T$, and $[1.2 \ 1.2 \ 0]^T$, respectively. The horizon size was set to $N = 7$. The noise covariances are given by $\mathcal{Q}_i = \text{diag}(0.1, 0.1, 0.1)$ and $\mathcal{R}_i = \text{diag}(0.01, 0.01, \dots, 0.01)$, where $i = 1, 2, \dots, 6$. The initial state covariance of the i -th robot was considered as $\mathcal{P}_{i,0} = \text{diag}(0.1 \ 0.1 \ 0.1)$, where $i = 1, 2, \dots, 6$.

The real trajectories and trajectories for the localization results with the DFMERM and the distributed IIR filter of 3-rd, 4-th, 5-th, and 6-th robots are shown in Figs. 4–7. Fig. 4 reveals that the localization performance of the distributed IIR filter is degraded in sections $29 \leq k \leq 33$ and $80 \leq k \leq 86$ where missing measurements occurred in the 3-rd robot. In addition, the 3-rd robot receives measurement values from the 6-th robot, where missing measurement occurred in $29 \leq k \leq 33$ and $75 \leq k \leq 79$, and the estimation error that occurred at those sections affected 3-rd robot. As a result, the section with the performance degradation appears longer than the section where the actual missing

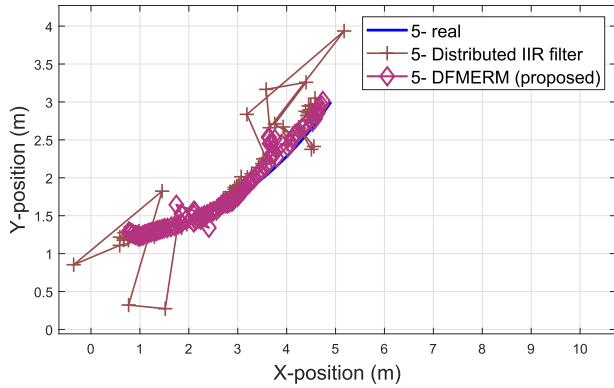


FIGURE 6. Robot 5 trajectory in the case of missing measurement.

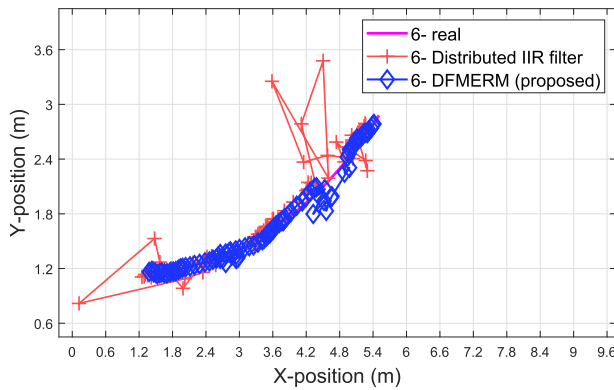


FIGURE 7. Robot 6 trajectory in the case of missing measurement.

measurement occurred. On the other hand, the proposed algorithm exhibits robust performance even in situations with missing measurements, and it can be confirmed that the output is close to the real value. Both the distributed IIR filter and proposed algorithm show similar performance, as shown in Fig. 5, except for one section where a measurement is missing for 4-th robot. The distributed IIR filter shows a large error in the section where a measurement is missing, and the performance deteriorates, whereas the output of the proposed algorithm approaches near the real value without large errors. The trajectories of 5-th and 6-th robots, where measurements were missing in the same $29 \leq k \leq 33$ and $75 \leq k \leq 79$ sections, are shown in Figs. 6-7, and the two robots are connected to each other in the network topology. Therefore, in a situation where measurements are missing, the estimated state of each robot affects each the performance of other robots. In particular, it can be seen that the estimated states of the 5-th and 6-th robots through the distributed IIR filter bounce in a similar direction with large errors, resulting in poor performance. The DFMERM shows robust performance, although the error increased compared to where a measurement was missing in 3-rd and 4-th robots.

Fig. 8 shows the estimation errors of both algorithms; A denotes the interval for $29 \leq k \leq 33$, B denotes the interval for $75 \leq k \leq 79$, and C denotes the interval for $80 \leq k \leq 86$. In interval A in Fig. 8, where all sensors are missing, we can see a large difference in the performance

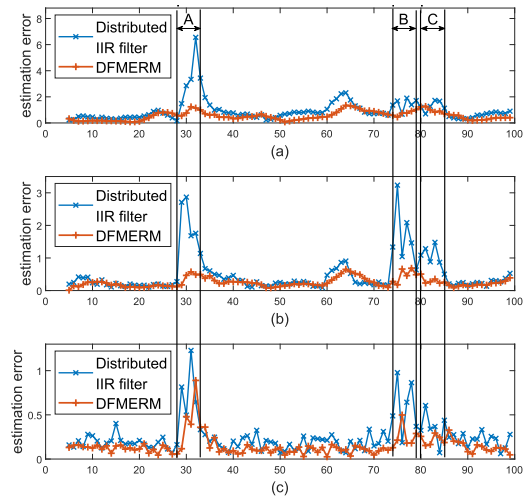


FIGURE 8. Sum of absolute estimation error results in the case of missing measurement: (a) x position (b) y position (c) heading angle.

TABLE 1. RMSE results.

		<i>x</i>	<i>y</i>	θ
missing	DFMERM	0.3451	0.2145	0.0412
measurement	Distributed IIR filter	0.7528	0.7462	0.1017

TABLE 2. Mean operation time.

		time (s)
missing	DFMERM	0.010
measurement	Distributed IIR filter	0.007

of both algorithms. In interval B, the sensors of the 5-th and 6-th robots were turned off, and in interval C the sensor of the 3-rd robot was turned off. Similarly, the robust performance of the DFMERM in intervals B and C in Fig. 8 is notable. The performance of error handling is clearly shown in Table 1 as root-mean-square error (RMSE) results. The DFMERM exhibited RMSE results that were more than two times lower. The distributed IIR filter periodically showed an error peak and divergence. However, in the DFMERM, the sum of the absolute estimation error did not grow rapidly and had small divergence. Therefore the DFMERM was more effective at handling missing measurement errors. The comparison of both filters with the average operation time in Table 2 was conducted in Raspberry Pi 3 B+ model with a 1.4GHz CPU. The average operation was approximately 1.4 times higher in DFMERM. However, the DFMERM can be used in real-time applications because both filters exhibited sufficiently low computational load.

B. APPEARANCE OF OBSTACLE CASE

In the second scenario, we considered the obstacle case where other robots could not be sensed. At $k = 120$, the 3-rd robot was kidnapped and placed on the opposite side of

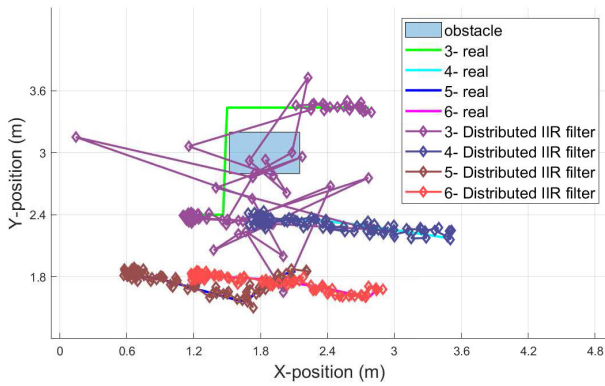


FIGURE 9. Robots trajectories with distributed IIR filter in the case of an obstacle.

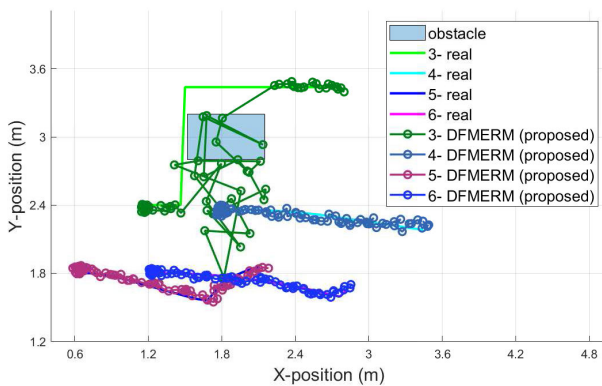


FIGURE 10. Robots trajectories with DFMERM in the case of an obstacle.

the obstacle. A total of 260 measurements were collected with $\Delta t = 0.5$ (s). We considered the topology network as $1 \rightarrow 5, 1 \rightarrow 3, 2 \rightarrow 4, 2 \rightarrow 6, 4 \rightarrow 3, 5 \rightarrow 6,$ and $6 \rightarrow 5$. The initial states of the 1-th, 2-th, \dots , 6-th robots are given as $[0.6 \ 2.4 \ 0]^T, [1.8 \ 1.8 \ 0]^T, [1.2 \ 2.4 \ 0]^T, [1.8 \ 2.4 \ 0]^T, [0.6 \ 1.8 \ 0]^T,$ and $[1.2 \ 1.8 \ 0]^T$, respectively. The horizon size was $N = 7$. Noise covariances and initial state covariances were set to be equal those in scenario 1.

The obstacle and real and estimated trajectory graphs are shown in Figs. 9 and 10, where both the distributed IIR filter and DFMERM exhibit poor performances when the 3-rd robot was kidnapped. In particular, in the distributed IIR filter, the error size changes drastically, whereas the proposed algorithm yielded a smaller error size. Moreover, as can be seen in Fig. 9, before and after the 3-rd robot was kidnapped and immediately after being kidnapping was over, the distributed IIR filter required some time-steps for stabilization, and continuous fluctuations were generated compared to the real value. However, Fig. 10 reveals that the proposed algorithm quickly and accurately approaches the real value immediately after the kidnapping was over.

The sum of the absolute estimation error is shown in Fig. 11; D denotes the interval where an obstacle appears.

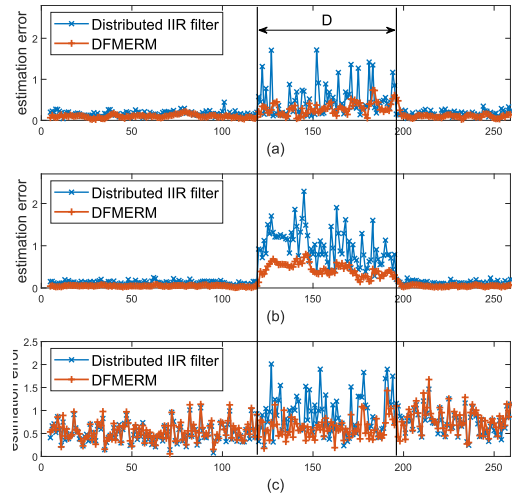


FIGURE 11. Sum of absolute estimation error results in the case of an obstacle: (a) x position (b) y position (c) heading angle.

TABLE 3. RMSE results.

		x	y	θ
appearance of obstacle	DFMERM	0.0451	0.0834	0.4499
	Distributed IIR filter	0.1281	0.3437	0.6213

TABLE 4. Mean operation time.

		time (s)
appearance of obstacle	DFMERM	0.011
	Distributed IIR filter	0.008

The error gradually increased during the kidnap in both filters. However, in the distributed IIR filter, starting with the attack, the error rapidly increased. The DFMERM was more than twice as effective as the distributed IIR filter when the error was at the peak for both filters. The RMSE results show that the DFMERM had approximately 2.8 and 4.7 times better performance, in terms of the x- and y-axes, than the distributed IIR filter, as shown in Table 3. As in the missing measurement case, the average operating time in Table 4 sufficiently indicates potential real-world applicability. Furthermore, according to the experimental results, the DFMERM is sufficiently applicable to WSNs in terms of robustness.

In addition to the experiments, a simulation was conducted to clarify the computational complexity. The simulation consisted of 25 nodes more robots than in the previous two experiments. The overall network topology for the simulation is shown in Fig. 12.

We assumed that the robots in nodes 1, 2, and 24 were in Group A, and their positions are estimated in a 2D plane in advance. The sampling interval was set to 0.1s, and the simulation was run up to 500 time steps. The average computational complexity during the simulation is shown in Table 5.

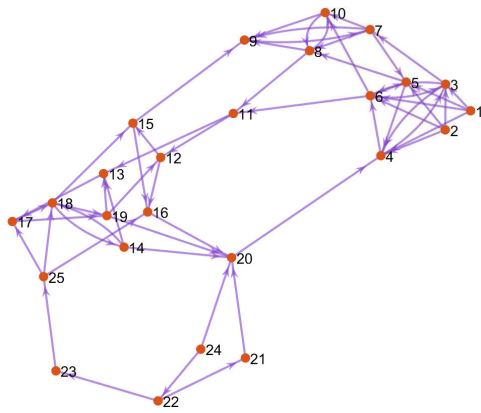


FIGURE 12. Simulation with 25 nodes with randomly initialized states.

TABLE 5. Mean operation time.

		time (s)
simulation	DFMERM	0.0061
	Distributed IIR filter	0.0044

The mean computational complexity of the distributed IIR filter was about 1.39 times faster than that of the proposed method, similar to in the previous experiments. However, the DFMERM had no difficulty in executing the algorithm in a loop within a given sampling time. Therefore, both experiments and the simulation confirmed that although the proposed algorithm is 1.4 times slower on average in terms of mean computational complexity than the distributed IIR filter, it can be implemented in a real-time experiment or simulation within the sampling time.

Remark 4: In the experiment involving an obstacle, only one obstacle was considered. When the number of obstacles increased, the obstacles interrupted communications between the robots and time delay occurred. This delay degraded the localization accuracy of both the DFMERM and the distributed IIR filter. Thus, it is required to study a new localization algorithm considering the time delay for the multiple-obstacle case.

V. CONCLUSION

In this paper, we proposed a novel distributed multiple-robot localization algorithm, namely, DFMERM. Due to the FM structure, the DFMERM has inherent robustness against modeling and computational errors. Moreover, the proposed algorithm overcomes the missing measurement problem by utilizing redefined measurements. The experimental results demonstrated that the DFMERM exhibited superior robustness against missing measurements and the sudden appearance of an obstacle compared with the conventional distributed IIR filter. We intend to apply the DFMERM to the 3D localization of unmanned aerial vehicles in future work.

REFERENCES

- [1] A. Yassin, Y. Nasser, M. Awad, A. Al-Dubai, R. Liu, C. Yuen, R. Raulefs, and E. Aboutanios, "Recent advances in indoor localization: A survey on theoretical approaches and applications," *IEEE Commun. Surveys Tuts.*, vol. 19, no. 2, pp. 1327–1346, 2nd Quart. 2016.
- [2] W. Ding, S. Chang, and J. Li, "A novel weighted localization method in wireless sensor networks based on hybrid RSS/AoA measurements," *IEEE Access*, vol. 9, pp. 150677–150685, 2021.
- [3] T. Wang, H. Ding, H. Xiong, and L. Zheng, "A compensated multi-anchors TOF-based localization algorithm for asynchronous wireless sensor networks," *IEEE Access*, vol. 7, pp. 64162–64176, 2019.
- [4] M. Akter, M. O. Rahman, M. N. Islam, M. M. Hassan, A. Alsanad, and A. K. Sangaiah, "Energy-efficient tracking and localization of objects in wireless sensor networks," *IEEE Access*, vol. 6, pp. 17165–17177, 2018.
- [5] J. M. Pak, C. K. Ahn, Y. S. Shmaliy, P. Shi, and M. T. Lim, "Accurate and reliable human localization using composite particle/FIR filtering," *IEEE Trans. Human-Mach. Syst.*, vol. 47, no. 3, pp. 332–342, Jun. 2017.
- [6] H. Liouane, S. Messous, O. Cheikhrouhou, M. Baz, and H. Hamam, "Regularized least square multi-hops localization algorithm for wireless sensor networks," *IEEE Access*, vol. 9, pp. 136406–136418, 2021.
- [7] Q. Qi, Y. Li, Y. Wu, Y. Wang, Y. Yue, and X. Wang, "RSS-AOA-based localization via mixed semi-definite and second-order cone relaxation in 3-D wireless sensor networks," *IEEE Access*, vol. 7, pp. 117768–117779, 2019.
- [8] J.-W. Zhu, Q. Wang, W.-A. Zhang, L. Yu, and X. Wang, "Sensor attack reconstruction for mobile robots via a switching Kalman fusion mechanism," *Nonlinear Dyn.*, vol. 102, no. 1, pp. 151–161, Sep. 2020.
- [9] B. Vaseghi, A. M. Pourmina, and S. Mobayen, "Secure communication in wireless sensor networks based on chaos synchronization using adaptive sliding mode control," *Nonlinear Dyn.*, vol. 89, no. 3, pp. 1689–1704, Aug. 2017.
- [10] T.-K. Chang, S. Chen, and A. Mehta, "Multirobot cooperative localization algorithm with explicit communication and its topology analysis," in *Robotics Research*. Cham, Switzerland: Springer, 2020, pp. 643–659.
- [11] S. Safavi, U. A. Khan, S. Kar, and J. M. F. Moura, "Distributed localization: A linear theory," *Proc. IEEE*, vol. 106, no. 7, pp. 1204–1223, Jul. 2018.
- [12] J. M. Pak, C. K. Ahn, P. Shi, Y. S. Shmaliy, and M. T. Lim, "Distributed hybrid particle/FIR filtering for mitigating NLOS effects in TOA-based localization using wireless sensor networks," *IEEE Trans. Ind. Electron.*, vol. 64, no. 6, pp. 5182–5191, Jun. 2017.
- [13] U. A. Khan, S. Kar, and J. M. F. Moura, "Distributed sensor localization in random environments using minimal number of anchor nodes," *IEEE Trans. Signal Process.*, vol. 57, no. 5, pp. 2000–2016, May 2009.
- [14] R. Olfati-Saber, "Distributed Kalman filtering for sensor networks," in *Proc. 46th IEEE Conf. Decis. Control*, Dec. 2007, pp. 5492–5498.
- [15] S. I. Roumeliotis and G. A. Bekey, "Collective localization: A distributed Kalman filter approach to localization of groups of mobile robots," in *Proc. IEEE Int. Conf. Robot. Automat.*, vol. 3, Apr. 2000, pp. 2958–2965.
- [16] S. I. Roumeliotis and G. A. Bekey, "Distributed multirobot localization," *IEEE Trans. Robot. Autom.*, vol. 18, no. 5, pp. 781–795, Oct. 2002.
- [17] S. S. Kia, S. F. Rounds, and S. Martinez, "A centralized-equivalent decentralized implementation of extended Kalman filters for cooperative localization," in *Proc. IEEE/RSJ Int. Conf. Intell. Robots Syst.*, Sep. 2014, pp. 3761–3766.
- [18] A. Gasparri, F. Pascucci, and G. Ulivi, "A distributed extended information filter for self-localization in sensor networks," in *Proc. IEEE 19th Int. Symp. Pers., Indoor Mobile Radio Commun.*, Sep. 2008, pp. 1–5.
- [19] G. Battistelli and L. Chisci, "Stability of consensus extended Kalman filter for distributed state estimation," *Automatica*, vol. 68, pp. 169–178, Jun. 2016.
- [20] O. Hlinka, O. Sluciak, F. Hlawatsch, P. M. Djuric, and M. Rupp, "Likelihood consensus and its application to distributed particle filtering," *IEEE Trans. Signal Process.*, vol. 60, no. 8, pp. 4334–4349, Aug. 2012.
- [21] J. Read, K. Achutegui, and J. Míguez, "A distributed particle filter for nonlinear tracking in wireless sensor networks," *Signal Process.*, vol. 98, pp. 121–134, May 2014.
- [22] H. Li and F. Nashashibi, "Cooperative multi-vehicle localization using split covariance intersection filter," *IEEE Intell. Transp. Syst. Mag.*, vol. 5, no. 2, pp. 33–44, Apr. 2013.
- [23] L. Yan, X. Zhang, Z. Zhang, and Y. Yang, "Distributed state estimation in sensor networks with event-triggered communication," *Nonlinear Dyn.*, vol. 76, no. 1, pp. 169–181, Apr. 2014.

[24] Y. Cai, J. Lu, O. H. Wang, and X. Xu, "The optimal distributed filtering for the coupled systems with random delay," *Nonlinear Dyn.*, vol. 70, no. 3, pp. 1711–1718, Nov. 2012.

[25] D. P. Kumar, T. Amgoth, and C. S. Rao Annavarapu, "Machine learning algorithms for wireless sensor networks: A survey," *Inf. Fusion*, vol. 49, pp. 1–25, Sep. 2019.

[26] T. L. T. Nguyen, F. Septier, H. Rajaona, G. W. Peters, I. Nevat, and Y. Delignon, "A Bayesian perspective on multiple source localization in wireless sensor networks," *IEEE Trans. Signal Process.*, vol. 64, no. 7, pp. 1684–1699, Apr. 2016.

[27] Z. Xiahou and X. Zhang, "Adaptive localization in wireless sensor network through Bayesian compressive sensing," *Int. J. Distrib. Sensor Netw.*, vol. 11, no. 8, Aug. 2015, Art. no. 438638.

[28] Y. Guo, B. Sun, N. Li, and D. Fang, "Variational Bayesian inference-based counting and localization for off-grid targets with faulty prior information in wireless sensor networks," *IEEE Trans. Commun.*, vol. 66, no. 3, pp. 1273–1283, Mar. 2018.

[29] S. H. You, J. M. Pak, C. K. Ahn, P. Shi, and M. T. Lim, "Unbiased finite-memory digital phase-locked loop," *IEEE Trans. Circuits Syst. II, Exp. Briefs*, vol. 63, no. 8, pp. 798–802, Aug. 2016.

[30] Y. S. Shmaliy, S. Zhao, and C. K. Ahn, "Unbiased finite impulse response filtering: An iterative alternative to Kalman filtering ignoring noise and initial conditions," *IEEE Control Syst. Mag.*, vol. 37, no. 5, pp. 70–89, Oct. 2017.

[31] S. S. Lee, D. H. Lee, D. K. Lee, H. H. Kang, and C. K. Ahn, "A novel mobile robot localization method via finite memory filtering based on refined measurement," in *Proc. IEEE Int. Conf. Syst., Man Cybern. (SMC)*, Oct. 2019, pp. 45–50.

[32] M. Vazquez-Olguin, Y. S. Shmaliy, and O. G. Ibarra-Manzano, "Distributed unbiased FIR filtering with average consensus on measurements for WSNs," *IEEE Trans. Ind. Informat.*, vol. 13, no. 3, pp. 1440–1447, Jun. 2017.

[33] S. Zhao, Y. S. Shmaliy, and C. K. Ahn, "Bias-constrained optimal fusion filtering for decentralized WSN with correlated noise sources," *IEEE Trans. Signal Inf. Process. Netw.*, vol. 4, no. 4, pp. 727–735, Dec. 2018.

[34] M. Vazquez-Olguin, Y. S. Shmaliy, and O. G. Ibarra-Manzano, "Distributed UFIR filtering over WSNs with consensus on estimates," *IEEE Trans. Ind. Informat.*, vol. 16, no. 3, pp. 1645–1654, Mar. 2020.

[35] J. M. Pak, C. K. Ahn, M. T. Lim, and M. K. Song, "Horizon group shift FIR filter: Alternative nonlinear filter using finite recent measurements," *Measurement*, vol. 57, pp. 33–45, Nov. 2014.

[36] J. M. Pak, C. K. Ahn, Y. S. Shmaliy, and M. T. Lim, "Improving reliability of particle filter-based localization in wireless sensor networks via hybrid particle/FIR filtering," *IEEE Trans. Ind. Informat.*, vol. 11, no. 5, pp. 1089–1098, Oct. 2015.

[37] J. M. Pak, C. K. Ahn, Y. S. Shmaliy, P. Shi, and M. T. Lim, "Switching extensible FIR filter bank for adaptive horizon state estimation with application," *IEEE Trans. Control Syst. Technol.*, vol. 24, no. 3, pp. 1052–1058, May 2016.



SANG SU LEE received the B.S. degree in electrical engineering from Korea University, Seoul, South Korea, in 2017, where he is currently pursuing the Ph.D. degree in electrical engineering with the Advanced Control Systems Laboratory. His research interests include robust control, distributed algorithms, system identification, and their application to networked multi-robot systems.



JUNG MIN PAK (Member, IEEE) received the B.S., M.S., and Ph.D. degrees in electrical engineering from Korea University, Seoul, South Korea, in 2006, 2008, and 2015, respectively. From 2016 to 2020, he was an Assistant Professor with the Department of Electrical Engineering, Wonkwang University, Iksan, Republic of Korea, where he is currently an Associate Professor with the Department of Electrical Engineering. His research interests include state estimation, target tracking, and localization.



CHOON KI AHN (Senior Member, IEEE) received the B.S. and M.S. degrees from the School of Electrical Engineering, Korea University, Seoul, South Korea, in 2000 and 2002, respectively, and the Ph.D. degree from the School of Electrical Engineering and Computer Science, Seoul National University, Seoul, in 2006. He is currently a *Crimson Professor of Excellence* with the College of Engineering and a Full Professor with the School of Electrical Engineering, Korea University. His current research interests include control, estimation, fuzzy systems, neural networks, and nonlinear dynamics. He was a recipient of the Early Career Research Award of Korea University, in 2015. In 2016, he was ranked #1 in Electrical/Electronic Engineering among Korean young professors based on research quality. In 2017, he received the *Presidential Young Scientist Award* from the President of South Korea. In 2020, he received the Outstanding Associate Editor Award for IEEE TRANSACTIONS ON NEURAL NETWORKS AND LEARNING SYSTEMS. In 2021, he received the Best Associate Editor Award for IEEE TRANSACTIONS ON SYSTEMS, MAN, AND CYBERNETICS: SYSTEMS. In 2019 and 2021, he received the Research Excellence Award from Korea University (Top 3% Professor of Korea University in Research).



YEONG JUN KIM received the B.S. degree from the School of Robotics, Kwangwoon University, Seoul, South Korea, in 2019, and the M.S. degree in electrical engineering from Korea University, Seoul, in 2021. His research interests include multi-robot systems, distributed control and estimation, finite impulse response filtering, model predictive control, event-triggered strategy, and containment control.



HYUN HO KANG received the B.S. degree in electrical engineering from Korea University, Seoul, South Korea, in 2017, where he is currently pursuing the Ph.D. degree with the School of Electrical Engineering. He was a Finalist in the Autonomous Drone Racing Competition of IEEE International Conference on Fuzzy Systems, in 2021. His research interests include optimal, robust, and intelligent controls for unmanned aerial vehicles (UAVs), and multi-agent systems.